Setting Up Experimental Bell Tests with Reinforcement Learning

Alexey A. Melnikov,[1] Pavel Sekatski,[1] and Nicolas Sangouard[1,2]
[1]Department of Physics, University of Basel, Klingelbergstrasse 82, 4056 Basel, Switzerland
[2]Institut de Physique Théorique, Université Paris Saclay, CEA, CNRS, F-91191 Gif-sur-Yvette, France

(Received 11 May 2020; accepted 8 September 2020; published 16 October 2020)

Finding optical setups producing measurement results with a targeted probability distribution is hard, as *a priori* the number of possible experimental implementations grows exponentially with the number of modes and the number of devices. To tackle this complexity, we introduce a method combining reinforcement learning and simulated annealing enabling the automated design of optical experiments producing results with the desired probability distributions. We illustrate the relevance of our method by applying it to a probability distribution favouring high violations of the Bell-Clauser-Horne-Shimony-Holt (CHSH) inequality. As a result, we propose new unintuitive experiments leading to higher Bell-CHSH inequality violations than the best currently known setups. Our method might positively impact the usefulness of photonic experiments for device-independent quantum information processing.

DOI: 10.1103/PhysRevLett.125.160401

Introduction.—Bell nonlocality is a remarkable feature that allows one to prove the incompatibility of an experiment with a classical description by assuming only no signaling and some form of independence between the experiment's devices [1]. First appreciated for its foundational implications, it was recently realized that Bell nonlocality is also a valuable resource to perform some quantum information tasks in a device-independent way, i.e., without ever assuming a detailed quantum model of the setup. This led to trustworthy protocols for quantum key distribution with device-independent security guarantees [2] and random number generation with device-independent randomness certifications [3]. In the same vein, self-testing [4] is the only technique that allows one to certify the functioning of quantum devices without assuming anything particular about their physical model.

In device-independent protocols, the quantity of interest, be it the rate of quantum key distribution, the randomness of outcomes, or the deviation from the ideal device in self-testing, is expressed as a scalar function of the probability distribution of measurement outcomes. In most cases, the targeted probability distribution is the one leading the highest Bell inequality violation. For example, the simplest and most studied Bell test is the Clauser, Horne, Shimony, and Holt (CHSH) test [5] which can be used for all aforementioned tasks. From a practical perspective, one of the main goals for performing device-independent quantum information tasks is, thus, to design an experiment with measurement outcomes optimizing the violation of the CHSH inequality.

With their high repetition rates and routinely controlled devices, optical experiments are appealing to perform a CHSH test as demonstrated in many experiments [6–11]. The CHSH inequality violations reported in these experiments are very small which prevents one from using them for most applications of device-independent quantum information processing. It is, thus, natural to wonder if the same optical devices can be rearranged to increase the CHSH inequality violations. Finding the setup leading to the highest CHSH score, that is, the highest CHSH inequality violation, is, however, not straightforward, as too many possibilities must be considered. It is the case that automation is becoming necessary to improve implementations of device-independent protocols.

Inspired by recent developments in machine learning [12–15], which is becoming more and more useful in automation of problem solving in quantum physics research [16–23], we introduce a technique based on the interplay between reinforcement learning [24] and simulated annealing [25] to design photonic setups maximizing a given function of probability distributions of measurement results. We illustrate the relevance of this method by applying it to probability distributions yielding high violations of the CHSH inequality with controlled resources. In essence, our algorithm not only rediscovered two known setups, but also discovered new, unexpected experimental settings leading to higher CHSH scores and, to our knowledge, are not analogous to any known settings.

CHSH test.—The way to realize the CHSH test is depicted in Fig. 1(a). A bipartite quantum state is prepared and shared between Alice and Bob. They then perform measurement on their system by randomly and independently choosing one out of two measurement settings: A_x with $x = 1, 0$ for Alice and B_y with $y = 0, 1$ for Bob. Each measurement has two possible outcomes ± 1 labeled a and b for Alice and Bob, respectively. The CHSH score is then computed from the distribution of measurement outcomes as

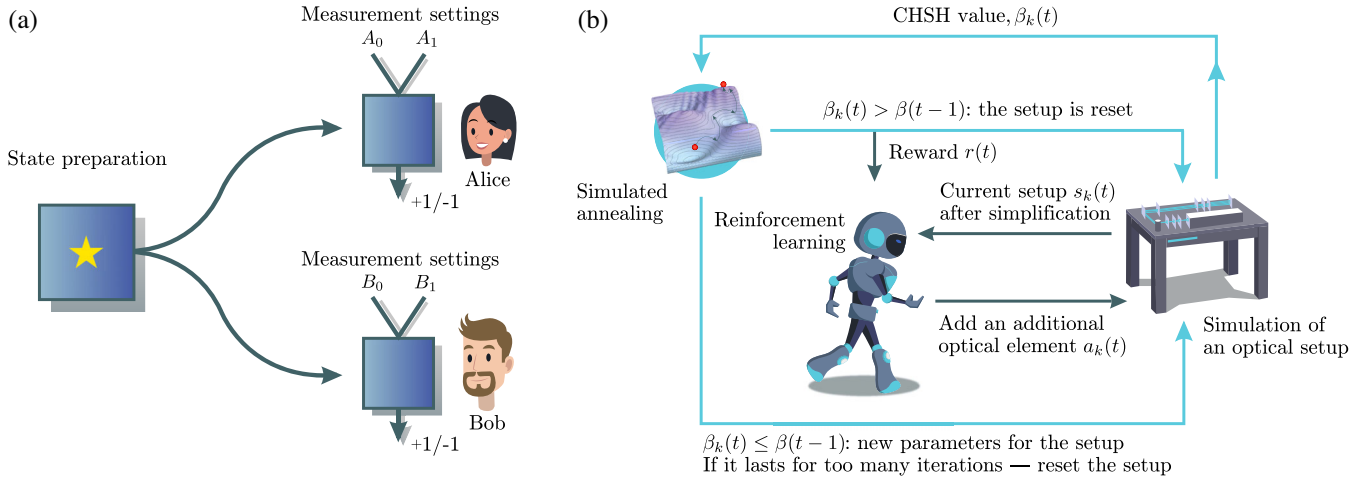

FIG. 1. (a) Schematic representation of a Bell test with two parties—Alice and Bob. In each round, Alice and Bob independently perform a measurement on the state that they share. The measurement outcomes that Alice and Bob observe by repeating the measurements are used to test a Bell inequality. (b) Schematic representation of the proposed learning protocol to design photonic experiments leading to a probability distribution of measurement outcomes favoring a large CHSH inequality violation. Reinforcement learning (gray-green arrows) and simulated annealing (blue arrows) approaches are used together.

$$\beta = \sum_{x,y=0}^{1} (-1)^{xy} [p(a = b|A_x B_y) - p(a \neq b|A_x B_y)], \qquad (1)$$

where $p(a = b|A_x B_y)$ is the probability that the results are the same given the setting choices A_x and B_y. Note that the CHSH score is upper bounded by 2 whenever there exists a locally causal model reproducing the measurement outcomes. The range of possible scores is enlarged to $|\beta| \leq 2\sqrt{2}$ with quantum models [26].

The physics of designed experiments.—We consider an experiment involving n bosonic modes initialized in the vacuum state. Their state is then manipulated by applying single-mode operations—phase shifters, displacement operations, and single-mode squeezers—and two-mode operations—beam splitters and two-mode squeezers—on any mode or pair of modes in any order or measuring out some of the modes with non-photon-number-resolving detectors; see Supplemental Material [27] for a detailed description of these elements. The state preparation is complete if the desired combination of outcomes *click* or *no click* is observed on $n - m$ detectors. The remaining m modes are shared between Alice and Bob, who locally apply a combination of operations from the same alphabet depending on their measurement settings. Finally, all the modes are measured out with non-photon-number-resolving detectors, yielding one of the 2^m possible outcomes. In our examples, we will consider the cases $\{m, n\} = \{2, 2\}$ and $\{2, 3\}$.

The alphabet of possible unitary operations we described is a fair representation of devices that are routinely used in optical experiments [45]. It is worth mentioning that degrees of freedom, such as polarization or frequency, are described by associating several bosonic modes to one photon. The use of a single-photon detector is motivated by the fact that the results of Gaussian operations alone can be reproduced by locally causal models.

Complexity.—To motivate an automated approach to our problem, let us discuss the complexity of finding the desired setup. *A priori*, the number of possible arrangements of elements grows exponentially with the number of modes and the total number of elements. However, as any combination of such elements defines a Bogolyubov transformation on the n modes, only $O(n^2)$ elements are needed; see Supplemental Material, Sec. B [27] for the details. Yet, an automated approach is very relevant for the design of such experiments for three reasons. First, the total number of parameters must also account for the measurement settings, and a brute-force approach would have to optimize the parameters of 23 elements for finding the highest CHSH score for the case $\{m, n\} = \{2, 3\}$. Second, if the elements include imperfections, the set of transformations which is accessible by combining individual elements is, in general, unknown, making a brute-force method unfeasible. Finally, a brute-force search is unsuitable when one is interested in keeping the number of elements low.

Learning to violate the CHSH inequality.—We now formalize the problem of an automated design of an optical setup leading to a high CHSH score as a reinforcement learning [24,46] task. The description of a setup we outlined before possesses two levels. The top level specifies the order in which different elements are applied on different modes. As each element is parametrized by one or more parameters, a second level specifies the value of these parameters. The automated design we propose treats the two levels on a very different footing—a learning agent focuses on the first level, and an optimization algorithm based on simulated annealing treats the second level.

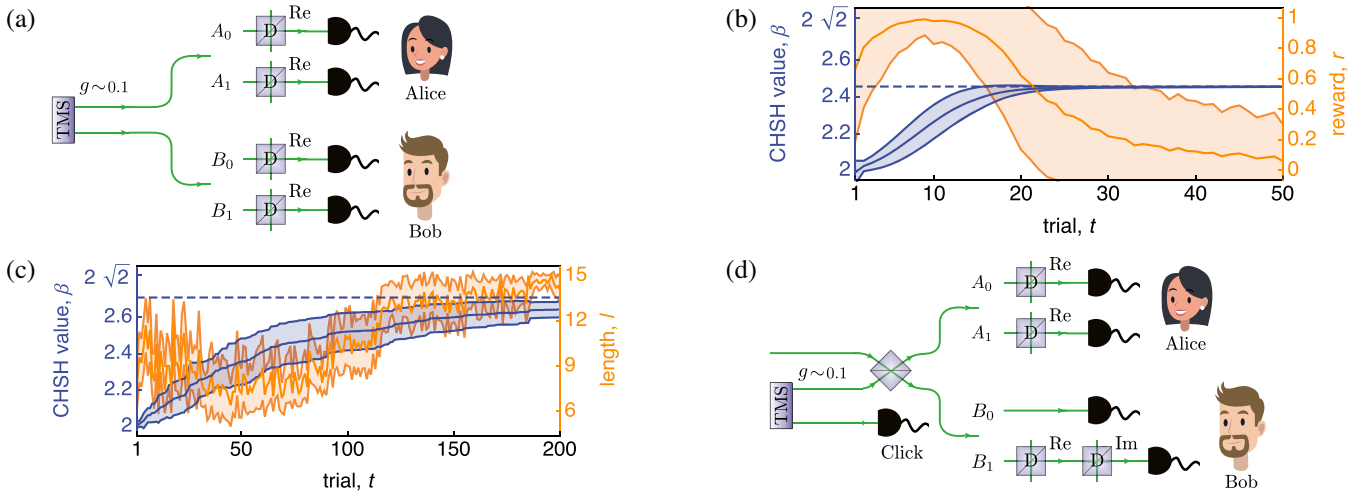

FIG. 2. (a) Setup used to test the reliability of the simulated annealing based optimization. Two modes, initially empty, are coupled by a two-mode squeezing (TMS) operation. One mode is sent to each party which he or she measures using photon detection preceded by displacement operations (D). (b) Learning curves reflecting the parameter optimization process performance for the fixed sequence shown in (a). The results are an average over 1000 independent runs, and shaded areas are mean squared deviations. $\beta \approx 2.4547$ (dashed line) is the optimal CHSH value found by using an analytical expression. (c) CHSH score and experiment length reflecting the reinforcement learning process of improving the CHSH value using a restricted set of elements. The results are an average over ten independent runs, and shaded areas are mean squared deviations. The maximal value of $\beta \approx 2.7075$ found by the learning agent is shown as a dashed line. (d) Setup combining simplicity and a relatively high CHSH score $\beta \approx 2.6401$ (the heralding probability is $p_{\text{click}} \approx 2.2 \times 10^{-3}$). The diamond shape element above the heralding detector is a beam splitter.

As seen in Fig. 1(b), the learning agent (shown as a robot) is interacting with a simulated experiment (shown as an optical table) in rounds or interaction steps. A sequence of interaction steps that leads to a feedback signal (reward) is called a trial. One interaction step is visualized in Fig. 1(b). At the beginning of each trial t, the agent perceives an input $s_1(t)$, which is a representation of an initial (empty) optical setup at the agent-environment interaction step $k = 1$. After a deliberation process, the agent chooses an optical element $a_1(t)$ (action) out of the set of available elements; see Fig. S1 in Supplemental Material [27] for the list of available elements. The chosen element is incorporated into the setup $s_1(t)$, and this combination makes up a new setup $s_2(t)$. The latter is then analyzed with the help of an optimization technique in order to understand the quality of the prepared setup. The optimization technique based on simulated annealing [25,47,48] tries to find the best parameters of all the chosen optical elements in the setup such that the measurement results lead to the highest possible CHSH score. The search for parameters runs until the maximum number of optimization iterations is reached or once the CHSH score at step k is higher than the previous best one $\beta(t-1) = \max_{k',t'} \beta_{k'}(t'|t' \leq t-1)$. If $\beta_k(t) > \beta(t-1)$, a reward of $r(t) = 1$ is given and the trial is finished: The agent starts the next trial from the initial configuration $s_1(t+1)$ with an updated CHSH score $\beta(t)$.

Optimizing a fixed setup.—The learning process relies on a good optimization algorithm that provides near-optimal CHSH values for each setup proposed by the agent. However, optimization is interrupted once the reward is determined to save more runtime on learning rather than optimization. Moreover, it is not important to determine the full capability of all the setups under consideration during the learning process. To learn, the agent needs only to figure out if the current setup is better than all the previous setups (with a high probability). To confirm this, we test the reliability of simulated annealing by first separating the optimization process from the reinforcement learning process. This is implemented by considering the fixed setup shown in Fig. 2(a). The learning scenario is equivalent to having a "lucky" agent that always chooses a setup known to produce a high CHSH score [49–51] or to an agent that already learned this setup.

Figure 2(b) shows the results of the parameter optimization in this scenario. In our protocol, the computation time allocated to the annealer increases with each subsequent trial. As a consequence, the CHSH score grows with the number of trials toward its maximum theoretical value (dashed line), which confirms that the optimization based on simulated annealing found near-optimal parameters. The maximum CHSH score found by the simulated annealing based optimization is $\beta \approx 2.4546$, which has only a 10^{-4} difference with the known optimal solution. Apart from the optimization procedure, it is important that a correct reward signal is paired with the dynamics of the CHSH score β. In Fig. 2(b), one can see that reward r is growing with time in parallel with β. However, the reward goes down toward zero with time, meaning that the agent receives nearly no feedback after 20 trials. This unusual

phenomenon, opposite to a standard scenario in reinforcement learning, where an agent is expected to keep maximizing the reward per trial, is explained by that fact that it becomes harder and harder to surpass the CHSH values of previous rounds once the CHSH score has nearly reached its maximum theoretical value.

Reinforcement learning with a limited set of devices.—We first start by considering a task in which the agent is given $n = 3$ bosonic modes and a restricted toolbox composed of beam splitters, two-mode squeezers, and displacement operations. Given that two modes will be distributed to Alice and Bob and the last one is detected, the agent is asked to design setups by getting feedback from simulated annealing.

As a reinforcement learning agent, we are using the projective simulation agent which was first introduced in Ref. [28] and since then was shown to be attractive both theoretically [29–32] and for practical use [33–35,46,52]. The details of the agent's internal structure and metaparameters are omitted here; see [27,53] for more information.

Figure 2(c) shows the evolution of the CHSH score and the length of the experiment $l(t)$, i.e., the evolution of the number of elements used by the agent per trial. One can see that the setup length first decreases before increasing. Similar to the behavior of the reward $r(t)$ observed in Fig. 2(b), it is hard to improve over nearly optimal solutions; hence, the agent gets no reward and, by gradually forgetting its previous experience, explores the most complex possibilities of the maximum allowed length $l_{\max} = 15$. The maximum length is set to avoid computational complexity in simulations and to avoid overcomplicated photonic setups that are difficult to realize experimentally. This maximum length is the same throughout our work and is lower than the number of $l = 23$ independent elements required for a general Bogolyubov transformation on the three modes; see Supplemental Material, Sec. B [27] for the details. As for the CHSH values, a setup is found leading to a maximum value of ∼2.7075 using 11 elements. Although the agent gets rewards more frequently when the CHSH score tends to increase, which may favor long lengths, he effectively gets a similar reward per action in shorter experiments with lower CHSH values. This trade-off can be controlled by the agent's metaparameters. When short length setups are favored, the agent finds frequently a simple setup leading to a CHSH score of ∼2.6401 in which modes 2 and 3 are first coupled with a two-mode squeezer and modes 1 and 2 are then coupled through a beam splitter; see Fig. 2(d). This corresponds to a physical implementation of a setup proposed in 1999 [54], where a CHSH inequality violation is observed by first sending a single photon into a beam splitter and measuring the output modes with photon detection preceded by displacement operations. Note that the agent is using displacements with real and imaginary parts; however, he does not use them symmetrically in the measurement choices. Each element with a complex parameter is indeed divided into two elements, one with a real parameter and one with a purely imaginary parameter, and the agent found a way to reduce the number of elements in the displacements from 8 to 4. This represents the internal feature of reinforcement learning agents—reducing the number of actions per reward, which corresponds to reducing the number of elements in setups.

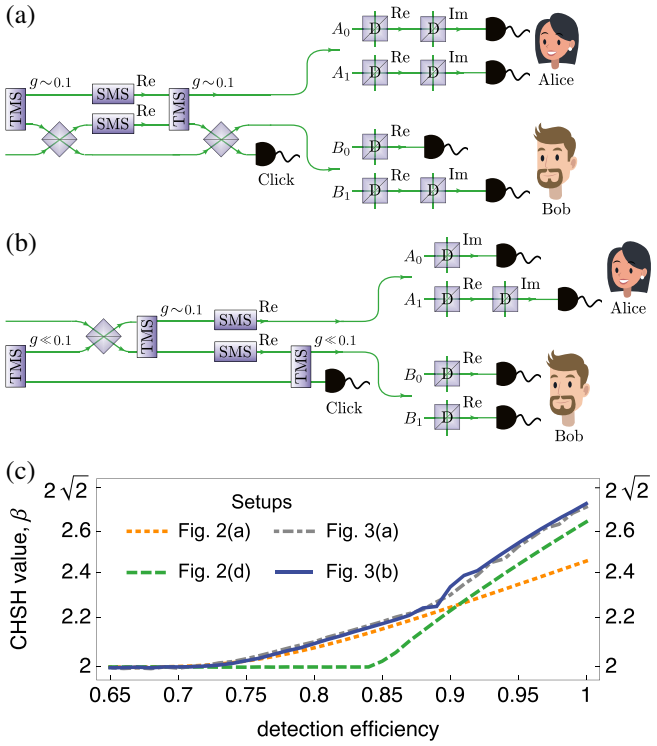

FIG. 3. Two photonic setups designed by the learning agent after learning from simpler examples. SMS elements correspond to single-mode squeezing operations. (a) A Bell test with CHSH score $\beta \approx 2.7242$ and a heralding probability $p_{\text{click}} \approx 2.9 \times 10^{-4}$, or $\beta \approx 2.7424$ with $p_{\text{click}} \approx 2.6 \times 10^{-5}$. (b) A Bell test with $\beta \approx 2.7454$ and $p_{\text{click}} \approx 1.1 \times 10^{-9}$. Parameters of the elements for both setups are in Supplemental Material [27]. (c) Dependence of the CHSH scores of setups which are considered in this work on detection efficiency. The setups designed by the agent provide higher CHSH values than known setups for any detection efficiency.

Proposal of new experiments with reinforcement learning.—Next, we allow the agent to choose between more elements by adding single-mode squeezing with a complex squeezing parameter to the previous set of elements. Benefiting from the extended space of possibilities, the agent gives us new setups, two of them producing CHSH scores above 2.74; see Figs. 3(a) and 3(b). We were not able to find known setups producing similar states. In order to witness the relevance of these new setups, we computed their CHSH score for nonunit detection efficiencies and reoptimized systematically the parameters of each element when the detection efficiency is changed.

For comparison, we also reported in Fig. 3(c) the CHSH score of setups shown in Figs. 2(a) and 2(d) which are known to be resistant to detector inefficiency and to produce high CHSH scores for close to unit efficiency detection respectively [55]. We conclude that the new setups provide higher CHSH scores for any detection efficiency. This can be partially understood by noting that the new setups have more elements and the possibility to control their parameters allows one to reduce them to setups close to the ones of Figs. 2(a) and 2(d). Although more detailed analyses are needed to conclude about the usefulness of these new setups in practice, they might provide additional motivations to develop programmable photonic integrated circuits.

Conclusion and outlook.—We have introduced a new learning approach to design photonic quantum experiments maximizing a desired function of the probability distribution of measurement outcomes. We observed that our learning agent is able to learn the experimental designs by trial and error. The agent was designing setups with increasing CHSH value and decreasing the experiment length whenever it was possible. As a result, new setups have been discovered with unprecedented CHSH values for any detection efficiency, which might positively impact the usefulness of photonic experiments for device-independent quantum information processing.

We are thankful to Enky Oudot, Xavier Valcarce, and Jean-Daniel Bancal for useful discussions. This work was supported by the Swiss National Science Foundation (SNSF), through Grant No. PP00P2-179109, and by the Army Research Laboratory Center for Distributed Quantum Information via the project SciNet. Computation was performed at sciCORE scientific computing core facility at University of Basel.

[1] N. Brunner, D. Cavalcanti, S. Pironio, V. Scarani, and S. Wehner, Rev. Mod. Phys. **86**, 419 (2014).
[2] R. Renner and A. Ekert, Nature (London) **507**, 443 (2014).
[3] M. Herrero-Collantes and J. C. Garcia-Escartin, Rev. Mod. Phys. **89**, 015004 (2017).
[4] I. Supic and J. Bowles, arXiv:1904.10042.
[5] J. F. Clauser, M. A. Horne, A. Shimony, and R. A. Holt, Phys. Rev. Lett. **23**, 880 (1969).
[6] M. Giustina, A. Mech, S. Ramelow, B. Wittmann, J. Kofler, J. Beyer, A. Lita, B. Calkins, T. Gerrits, S. W. Nam *et al.*, Nature (London) **497**, 227 (2013).
[7] B. G. Christensen, K. T. McCusker, J. B. Altepeter, B. Calkins, T. Gerrits, A. E. Lita, A. Miller, L. K. Shalm, Y. Zhang, S. W. Nam *et al.*, Phys. Rev. Lett. **111**, 130406 (2013).
[8] L. K. Shalm, E. Meyer-Scott, B. G. Christensen, P. Bierhorst, M. A. Wayne, M. J. Stevens, T. Gerrits, S. Glancy, D. R. Hamel, M. S. Allman *et al.*, Phys. Rev. Lett. **115**, 250402 (2015).
[9] M. Giustina, M. A. M. Versteegh, S. Wengerowsky, J. Handsteiner, A. Hochrainer, K. Phelan, F. Steinlechner, J. Kofler, J.-A. Larsson, C. Abellán *et al.*, Phys. Rev. Lett. **115**, 250401 (2015).
[10] L. Shen, J. Lee, L. P. Thinh, J.-D. Bancal, A. Cerè, A. Lamas-Linares, A. Lita, T. Gerrits, S. W. Nam, V. Scarani, and C. Kurtsiefer, Phys. Rev. Lett. **121**, 150402 (2018).
[11] Y. Liu, Q. Zhao, M.-H. Li, J.-Y. Guan, Y. Zhang, B. Bai, W. Zhang, W.-Z. Liu, C. Wu, X. Yuan *et al.*, Nature (London) **562**, 548 (2018).
[12] Y. LeCun, Y. Bengio, and G. Hinton, Nature (London) **521**, 436 (2015).
[13] J. Schmidhuber, Neural Netw. **61**, 85 (2015).
[14] V. Mnih, K. Kavukcuoglu, D. Silver, A. A. Rusu, J. Veness, M. G. Bellemare, A. Graves, M. Riedmiller, A. K. Fidjeland, G. Ostrovski *et al.*, Nature (London) **518**, 529 (2015).
[15] D. Silver, T. Hubert, J. Schrittwieser, I. Antonoglou, M. Lai, A. Guez, M. Lanctot, L. Sifre, D. Kumaran, T. Graepel *et al.*, Science **362**, 1140 (2018).
[16] V. Dunjko and H. J. Briegel, Rep. Prog. Phys. **81**, 074001 (2018).
[17] G. Carleo, I. Cirac, K. Cranmer, L. Daudet, M. Schuld, N. Tishby, L. Vogt-Maranto, and L. Zdeborová, Rev. Mod. Phys. **91**, 045002 (2019).
[18] J. Biamonte, P. Wittek, N. Pancotti, P. Rebentrost, N. Wiebe, and S. Lloyd, Nature (London) **549**, 195 (2017).
[19] V. Dunjko and P. Wittek, Quantum Views **4**, 32 (2020).
[20] A. A. Melnikov, L. E. Fedichkin, and A. Alodjants, New J. Phys. **21**, 125002 (2019).
[21] A. A. Melnikov, L. E. Fedichkin, R.-K. Lee, and A. Alodjants, Adv. Quantum Technol. **3**, 1900115 (2020).
[22] J. Jašek, K. Jiráková, K. Bartkiewicz, A. Černoch, T. Fürst, and K. Lemr, Opt. Express **27**, 32454 (2019).
[23] G. Marcucci, D. Pierangeli, P. W. H. Pinkse, M. Malik, and C. Conti, Opt. Express **28**, 14018 (2020).
[24] R. S. Sutton and A. G. Barto, *Reinforcement Learning: An Introduction*, 2nd ed. (MIT Press, Cambridge, MA, 2018).
[25] P. J. Van Laarhoven and E. H. Aarts, in *Simulated Annealing: Theory and Applications* (Springer, New York, 1987), pp. 7–15.
[26] B. Cirel'son, Lett. Math. Phys. **4**, 93 (1980).
[27] See Supplemental Material at http://link.aps.org/supplemental/10.1103/PhysRevLett.125.160401 for details about optical elements and optical setups, and a more detailed description of the reinforcement learning algorithm. Sec. A, which includes Refs. [28–40,46], and Sec. B, which includes Refs. [41–44].
[28] H. J. Briegel and G. De las Cuevas, Sci. Rep. **2**, 400 (2012).
[29] J. Mautner, A. Makmal, D. Manzano, M. Tiersch, and H. J. Briegel, New Gener. Comput. **33**, 69 (2015).
[30] A. Makmal, A. A. Melnikov, V. Dunjko, and H. J. Briegel, IEEE Access **4**, 2110 (2016).
[31] A. A. Melnikov, A. Makmal, V. Dunjko, and H. J. Briegel, Sci. Rep. **7**, 14430 (2017).
[32] J. Clausen, W. L. Boyajian, L. M. Trenkwalder, V. Dunjko, and H. J. Briegel, arXiv:1910.11914.
[33] S. Hangl, E. Ugur, S. Szedmak, and J. Piater, in *Proceedings of the IEEE/RSJ International Conference*

on Intelligent Robots and Systems (IEEE, New York, 2016), pp. 2799–2804.
[34] A. A. Melnikov, A. Makmal, and H. J. Briegel, IEEE Access **6**, 64639 (2018).
[35] J. Wallnöfer, A. A. Melnikov, W. Dür, and H. J. Briegel, PRX Quantum **1**, 010301 (2020).
[36] M. Krenn, M. Malik, R. Fickler, R. Lapkiewicz, and A. Zeilinger, Phys. Rev. Lett. **116**, 090405 (2016).
[37] P. A. Knott, New J. Phys. **18**, 073033 (2016).
[38] L. O'Driscoll, R. Nichols, and P. A. Knott, Quantum Mach. Intell. **1**, 5 (2019).
[39] R. Nichols, L. Mineh, J. Rubio, J. C. F. Matthews, and P. A. Knott, Quantum Sci. Technol. **4**, 045012 (2019).
[40] M. Krenn, M. Erhard, and A. Zeilinger, arXiv:2002.09970.
[41] M. Reck, A. Zeilinger, H. J. Bernstein, and P. Bertani, Phys. Rev. Lett. **73**, 58 (1994).
[42] B. He, J. A. Bergou, and Z. Wang, Phys. Rev. A **76**, 042326 (2007).
[43] G. Adesso, S. Ragy, and A. R. Lee, Open Syst. Inf. Dyn. **21**, 1440001 (2014).
[44] C. Weedbrook, S. Pirandola, R. García-Patrón, N. J. Cerf, T. C. Ralph, J. H. Shapiro, and S. Lloyd, Rev. Mod. Phys. **84**, 621 (2012).
[45] The implementation of higher order interaction is way more demanding and inefficient.
[46] A. A. Melnikov, H. Poulsen Nautrup, M. Krenn, V. Dunjko, M. Tiersch, A. Zeilinger, and H. J. Briegel, Proc. Natl. Acad. Sci. U.S.A. **115**, 1221 (2018).
[47] A. G. Nikolaev and S. H. Jacobson, in *Handbook of Metaheuristics* (Springer, New York, 2010), pp. 1–39.
[48] D. Pham and D. Karaboga, *Intelligent Optimisation Techniques* (Springer Science & Business Media, New York, 2012).
[49] A. Kuzmich, I. A. Walmsley, and L. Mandel, Phys. Rev. Lett. **85**, 1349 (2000).
[50] S.-W. Lee, H. Jeong, and D. Jaksch, Phys. Rev. A **80**, 022104 (2009).
[51] J. B. Brask and R. Chaves, Phys. Rev. A **86**, 010103(R) (2012).
[52] H. Poulsen Nautrup, N. Delfosse, V. Dunjko, H. J. Briegel, and N. Friis, Quantum **3**, 215 (2019).
[53] Projective simulation Github repository, github.com/qic-ibk/projectivesimulation, accessed: 2020-04-05.
[54] K. Banaszek and K. Wódkiewicz, Phys. Rev. Lett. **82**, 2009 (1999).
[55] V. C. Vivoli, Université de Genève, Ph.D. thesis, 2015.